Send Orders of Reprints at reprints@benthamscience.net

Anti-Cancer Agents in Medicinal Chemistry, **2013**, *13*, **1-12** **1**

Cancer Antibody Enhanced Real Time Imaging Cell Probes – a Novel Theranostic Tool

Gerda Brakmane[1], Seyed Yazdan Madani[1] and Alexander Seifalian[1,2,3,*]

[1]*Centre for Nanotechnology & Regenerative Medicine, UCL Division of Surgery & Interventional Science, University College London, London, UK;* [2]*Royal Free Hampstead NHS Trust Hospital, London, UK;* [3]*London Centre of Nanotechnology, London, UK*

Abstract: *Background*: Cancer is a potentially fatal diagnosis, but due to modern medicine there is a potential cure in many of these cases. The rate of treatment success depends on early disease detection and timely, effective delivery of tumour specific treatment. There are many ongoing researches aimed to improve diagnostics or treatment, but the option to use both modalities concomitantly is deficient. In this project we are using the advances in nanotechnology to develop new theranostic tool using single walled carbon nanotubes (SWCNT) and Quantum dots (QDs) for early cancer cell detection, and option to deliver targeted treatment.

Method: SWCNTs were refluxed in HNO3/H2SO4 (1:3) at 120ºC for 120 minutes. Functionalised SWCNT was then covalently attached to octa-ammonium polyhedral oligomeric silsesquioxane (POSS), QDs and conjugated with antibodies for targeted cell detection. Fourier transforms infrared spectroscopy (FTIR), Transmission electron microscopy (TEM), UV/NIR analysis, Raman and UV-VIS spectroscopy were used in order to prove the successful conjugation. Toxicology study using alamar blue analysis and DNA assay was conducted in order to choose the best concentration of SWCNT, octa-ammonium-POSS and QDs before commencing the conjugation process. Human colorectal cancer cell line HT29, pancreas cancer cell line PANC-1 and mouse fibroblasts 3T3 were then treated with or without antibody conjugated SWCNT-POSS-QDs (CPQ) compound solution. The cell response was observed under the microscope after 24, 48 and 72 hours.

Results: FTIR and Raman spectroscopies confirmed covalent binding of the SWCNTs to Octa-Ammonium-POSS. This was supported by TEM images and photos obtained, which showed well dispersed SWCNTs following its treatment with Octa-Ammonium-POSS compared to pristine SWCNT samples. UV-VIS graphs determined the presence of antibody within the compound. UV/NIR demonstrated QD fluorescence even after attachment of SWCNT-POSS. The cellular behaviour revealed high CPQ-antibody complex affinity towards cancer cells when compared to healthy cell line which internalised the complex only on day three. The pancreas cancer cell line had appearance of lysed pulp after 72 hours of incubation. Colonic cancer cells seemed to regain ability to populate from day three signifying that higher treatment payload is necessary.

Conclusion: We have successfully manufactured novel compound consisting of Octa-Ammonium-POSS linked SWCNTs, QDs, and tumour specific antibodies. The complex has proven its potential as cell probing tool, and the attachment of antibodies has shown high affinity to cancer cells rendering this an attractive model for further theranostic developments.

Keywords: ??????????

INTRODUCTION

Bowel cancer is the third most common cancer in UK with incidence approximating 40,000 per year. Pancreatic cancer although not as common (UK incidence approx. 8,000/yr), but due to late detection and aggressive cancer nature is far more difficult to treat. The mainstay of treatment involves surgical removal of cancerous tissue with anti-tumour medication often given before or after surgery. Current chemotherapeutic treatments consist of high doses of toxic drugs with severe systemic side effects. Nanotechnology holds promise in this regard by offering drug delivery by miniscule particles with large surface area to volume ratio thus reducing requirements of drug payload [1]. In case of oncology where clinical outcomes depend on timely disease detection and rapid initiation of treatment, this project outlines proposition of combining both. The aim of this project is to develop bio-compatible single walled carbon nanotubes (SWCNT) conjugated with quantum dots (QDs) for real-time cancer cell detection and option for concomitant delivery of chemotherapeutic agent which could be loaded into the SWCNTs or attached on pre-functionalised SWCNT surface. Successful creation of biocompatible fluorescent nanosystems for concurrent *in vivo* imaging and drug delivery would enable this approach to be examined for uses other than oncology. QDs and SWCNT conjugates offer added advantage for potential use in photodynamic therapy [2].

*Address correspondence to this author at the Professor of Nanotechnology & Regenerative Medicine, University College London; Tel: +44 20 7830 2901; E-mail: a.seifalian@ucl.ac.uk

CNTs consist entirely of carbon atoms, and due to high aspect ratio and unique electro-mechanical properties they have gained enormous interest as drug delivery platforms. SWCNT are made of rolled-up solitary graphene sheets whereas multi walled carbon nanotubes (MWCNT) consist of two or more concentric layers of the former [3]. In comparison to MWCNT the SWCNTs have been shown to exhibit higher cytotoxicity depending on concentration and exposure time [4]. Their pattern of entering cells has been described as 'needle-like' [5, 6]. The passive cellular internalisation process has been studied on various cell lines, and concerns of similarities to asbestos toxicity have been raised [7]. It has, however been proven that that acute inflammatory response is nanotube length-dependent, and unremitting inflammation and formation of granulomas and fibrosis results from exposure to nanotubes beyond 10μm long [8]. In contrast shorter CNTs have not shown to instigate such cytotoxicity making them attractive intracellular drug delivery vehicles that can be eliminated *via* natural immunological pathways [9].

QDs are semi-conductive nanocrystals with very long half-life and wide size dependent fluorescence spectrum. They consist of metallic crystal core, inorganic shell and can have coating of various materials. The crystal core often has defects on its surface leading to intermittent fluorescence (known as 'blinking'); therefore shell is overlapped to overcome this issue [10]. In addition, shell reduces the toxic effects when heavy metal ions (Cd, Zn, Pb) bind to cell membranes and intracellular proteins causing production of free radicals that triggers cytotoxic reactions [11, 12]. When irradiated with ultraviolet beam, QDs emit light that can be seen with naked eye. Conventional histology dyes fade over short period

1871-5206/13 $58.00+.00 **© 2013 Bentham Science Publishers**

of time and require tissue fixation *ex vivo*. QDs are more advantageous offering real-time *in vivo* imaging at molecular, cellular and tissue level [13]. Nano scaled polymers are used in nano sciences for development of new drug delivery tools and tissue-engineered scaffolds [14, 15]. In the past few years a novel polymer - polyhedral oligomeric silsesquioxane (POSS) has become evident. This adaptable and highly biocompatible polymer has already shown great potential in tissue engineering with evidence of clinical benefits. It has shown remarkable potential in generation of aortic and small vascular grafts [16, 17], lacrimal apparatus [18] and as scaffold for organogenesis [19]. The most outstanding example of its numerous applications is tissue-engineered tracheobronchial scaffold which has already been transplanted in human recipient with great success [20]. Octa-ammonium polyhedral oligomeric silsesquioxane (POSS) is a subtype of POSS with eight free amine groups rendering this polymer a desirable and versatile platform for further modifications. Due to readily available amine groups it is ideal for reactions with carboxyl groups that are found on SWCNTs and QDs to form strong covalent bonds, and increase the biocompatibility of the latter two. Current clinical practice often utilises cancer antibodies as part of cancer detection pathway and for estimation of treatment success. These large molecules made up of protein with light and heavy chains (exposed amine and carboxyl groups, respectively) make them amenable for conjugation with corresponding group-carrying substances. It has been shown in previous studies that antibodies used in common clinical practice can be functionalised onto nano platforms to aid specificity of cell detection and target delivery of treatment [21-23].

MATERIALS AND METHODS

Experimental Agents

Experimental agents 3-dimethylaminopropyl-N-ethylcarbodiimide hydrochloride (EDC) (99%), H_2SO_4 (95%), HNO_3 (70%), 4% paraformaldehyde, N-hydroxysuccinimide (NHS), L-Glutamine-penicillin-streptomycin solution along with monoclonal anti-human carcinoembryonic antigen (CEA) and human pancreatic adenocarcinoma cell line (PANC-1) were purchased from Sigma Aldrich (Dorset, UK). Phosphate buffered saline (PBS), bovine serum albumin (BSA), fetal calf serum (FCS), Dulbecco's modified Eagle's medium (DMEM), trypsin (0.5 g/L), AlamarBlue® reagent, Quant-iT™ PicoGreen® DNA assay, human colonic adenocarcinoma cell line (HT-29) and mouse fibroblast cell line 3T3 were purchased from Invitrogen™ (Paisley, UK). Monoclonal anti-CA 19-9 antibody was purchased from Abcam® (Cambridge, UK). Octa-ammonium polyhedral oligomeric silsesquioxanes (POSS) was purchased from Hybrid Plastics® (Hattiesburg, USA).

Preparation of Carboxyl-functionalised SWCNTs

Solid SWCNTs in powder form were purchased from Sigma Aldrich. The purity of SWCNTs used was 50-70 vol%, the diameter and length ranges were 1.2-1.5 nm × 2-5 μm, respectively. 10 mg of SWCNTs was dispersed in 30 mL of 1:3 HNO_3 : H_2SO_4 solution, refluxed at 120^{0}C for 120 minutes stirring at 500 rpm. The mixture was then centrifuged for 30 minutes at 2400 x g, and sonicated for 1 hour (Telsonic sonic bath, Switzerland). SWCNTs were expansively washed in deionised water until constant pH of 5-6 was reached.

Synthesis of SWCNT and Octa-Ammonium-POSS Conjugate

3 mg of SWCNTs was mixed with 1.5mg EDC and 0.9mg NHS, dissolved in 3 mL of DMF, and stirred at room temperature for 2 hours. This step is necessary to separate SWCNTs, and when mixed with Octa-Ammonium-POSS will enable polymer expansion.

Process was followed by ultrasonication for 3 minutes at room temperature (750-Watt Ultrasonic Homogenizer with Temperature Controller, 230 VAC, Cole-Parmer®, London, UK) to improve SWCNT dispersion. 3 mg of Octa-Ammonium-POSS was dissolved in 1 ml of 1M NaOH (premade of 4 g NaOH pellets dissolved in 100 mL water), which changes its –NH3 group to –NH2 improving reactions with –COOH groups.

SWCNT and Octa-Ammonium-POSS solutions were mixed together and stirred at room temperature for 1 hour. Mixture was then taken and centrifuged using 100 kDa filter system (Amicon ultra-4 centrifugal filter unit, Sigma Aldrich) at room temperature for 15 minutes at 5000 rpm (Centrifuge Mistral 3000i, MSE, London, UK). Distilled water was added to precipitate, and centrifuge cycle repeated. Final precipitate was oven dried for 10 minutes at 68^{0}C, and dried weight calculated. PBS was then added to obtain 1mg/ml concentration.

Synthesis of SWCNT-Octa-Ammonium-POSS and QDs Conjugate

Zinc and cadmium core quantum dots (QDs) with free surface –COOH groups, and emission spectrum of 600 nm were used (Fig. **1**). QDs solution was mixed with methanol at 1:1 volume ratio, and centrifuged for 5000 rpm at room temperature for 10 minutes. Supernatant was then discarded, and PBS added to weighed precipitate to obtain 1mg/ml concentration. QDs and SWCNT-Octa-Ammonium-POSS solutions were combined to make up final solution of 1:1 concentration ratio.

Cell Culture

Human colonic adenocarcinoma cell line HT-29 was grown in growth media (DMEM with 10% v/v FBS and 1% v/v L-Glutamine-penicillin-streptomycin antibiotic solution) at 37^{0}C 5% CO_2 incubator until 80-90% confluence was achieved on the bottom of 75 cm^2 flask. Cells were then removed from growth media, washed with PBS three times and incubated at 37^{0}C for 3 minutes after adding 2ml of 0.5g/l trypsin. After cells were detached from the flask 10 ml of fresh growth media was added and centrifuged for 5 minutes at 1500 rpm (Centrifuge PK120, ALC International Srl., Italy). Supernatant was then discarded and cell pellet dissolved in 5 ml growth media. Trypan blue assay (Sigma Aldrich) was used to establish viable cell count.

Toxicity experiment was modelled to determine cellular response to varying concentrations of SWCNTs, QDs and Octa-Ammonium-POSS. 96-well plates were prepared for the test with cell density 5000 cells per well. 100 μL SWCNT, QDs and Octa-Ammonium-POSS solutions were added to each well with concentrations from 0 to 1.0 mg/ml at 0.1 mg/ml increments to study cell response 24, 48 and 72 hours after incubation. Viability and metabolic activity were studied using Quant-iT™ PicoGreen® DNA assay and AlamarBlue® assay. Obtained data were statistically processed. From the acquired data the least toxic concentrations of SWCNT, QDs and Octa-Ammonium-POSS were selected, and the complex was prepared as per protocol above for further experiments.

Metabolic Activity Assay

Metabolic activity was assessed on three consecutive days. The AlamarBlue® kit was used for this test, and prepared as per Invitrogen™ protocol. A 100 μl reagent was added to each well; plates were then covered with foil and incubated at 37^{0}C. After 3 hours the samples were transferred to corresponding wells on black 96-well plates, and placed in fluorescence reader (Fluoroskan Ascent FL, Thermo Fisher Scientific Inc., Waltham, MA, US) using 530 nm wavelength of excitation and 620 nm emission. The obtained data were statistically analysed.

DNA Assay

In preparation for DNA assay, samples underwent three freeze-thawing cycles. A 100μl of distilled H_2O was added to each well,

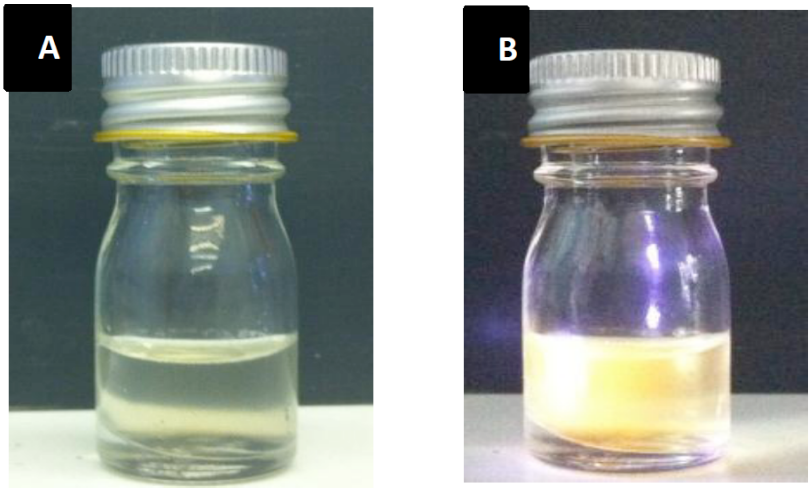

Fig. (1). Quantum dots as seen in daylight (**A**) and after application of UV light (**B**).

and samples were placed in -80^{0}C freezer for 30 min, followed by incubation at 37^{0}C for 30 min (cycle repeated three times). All assay components were prepared as per Invitrogen™ protocol for Quant-iT™ PicoGreen® DNA assay. A 100 µl of buffer solution was added to each well; samples were then transferred to corresponding wells of black 96-well plates along with prepared standard solutions. Cell viability using DNA assay was assessed on three consecutive days. Sample fluorescence was then measured using fluorometer (wavelength of excitation 485 nm, emission 538 nm), and data statistically processed.

Statistical Analysis

Quantitative data were expressed as the mean + standard deviation. Means were compared using independent-samples Kruskal-Wallis test with SPSS 17.0 software (SPSS Inc, Chicago, IL). The p-value of 0.05 was considered to be statistically significant.

Attachment of Antibodies to SWCNT-Octa-Ammonium-POSS Conjugated QDs

10 µl CEA and anti-CA 19-9 antibody concentrates were diluted into two separate containers with 1ml of antibody Diluent Dako REAL™ (Ely, UK). To 1 ml of SWCNT-Octa-Ammonium-POSS-QDs complex, 5 mg of NHS and 5 mg EDC was added, and placed on shaker (KS 10, Edmund Bühler GmbH, Germany) at speed 50 for 20 minutes at room temperature. 100 µL of each diluted antibody solution was added to SWCNT-Octa-Ammonium-POSS-QDs complex, and placed on shaker at speed 30 for 10 minutes at room temperature. Mixtures were then centrifuged using 100 kDa filter system at room temperature for 10 minutes at 5000 rpm. Supernatant was discarded, PBS added to pre-marked level and then mixed. Further on the two solutions with attached antibodies CEA and CA 19-9 will be referred to as CPQ-CEA and CPQ-CA, respectively.

Cell Culture and Staining

PANC-1, HT-29 and mouse fibroblast cell line 3T3 were grown and cultured as per protocol described above, and cell count established using Trypan blue. 24-well plates were seeded with HT-29, PANC-1 and 3T3 cell cultures (seeding density 2500 per well), and supplemented with growth medium. After 24 hours of incubation at 37^{0}C, 5% CO_2 conditions growth media, CPQ without antibodies or CPQ+antibody was added into the plates to be examined after three consecutive days. On the day of experiment, 24-well plates were removed from incubator and cells were washed three times with PBS to remove free CPQ complexes. A 200µl of HistoChoice® (Tissue Fixative, Sigma Aldrich) was added per well. After 20 minutes, cells were washed three times with PBS. To increase membrane permeability prior staining, a 200 µl of 0.1% Triton®X-100 (Sigma Aldrich) was added, and cells washed three times with PBS after 10 minutes. A drop of Vectashield® mounting medium with propidium iodide (Vector Laboratories, Burlingame, CA, US) was added to each well, and samples examined using confocal microscopy.

CONTENTS OF THE RESULTS

UV-VIS

UV-VIS spectrometry (V-630, JASCO, Easton, MD, US) was used to detect absorbance spectrum of CPQ complex and its components. SWCNT absorbance peaks were detected at 500 and 730 nm wavelengths when examined in PBS solution. After adding Octa-Ammonium-POSS to the SWCNT, absorbance of the latter remained unchanged; this could be explained with difficulties to uniformly coat the CNTs with polymer. QDs in PBS were compared to CNTs alone and revealed similar absorbance spectra. The CPQ-antibody complexes revealed presence of proteins within the complex with wide wavelengths at 260 nm.

UV/NIR

Literature evidence suggests that covalently functionalised CNTs are better for drug delivery and gene therapy, but not ideal as imaging platform [24]. The CPQ complex consists of covalently bound ingredients; therefore UV/NIR spectroscopy (ENFIS Unolight ngine, Photonstar Technology Limited, Romsey, UK) was performed to investigate CNT photobleaching effects on QDs. For experiment, QDs with 600 nm emission spectrum were used. Polymer alone emitted a weak signal at 550 nm range, but in combination with QD it did not prove to affect strong emission signal of the latter. The –COOH functionalised CNTs alone failed to emit a signal even at NIR spectrum. When covalently bound to QDs through attachment of POSS, CNTs reduced but did not abolish the signal amplitude of QDs (Fig. **2**).

FTIR

Fourier transform infrared spectrometer (FT/IR-4200, JASCO, Easton, MD, US) was used. The test was chosen to confirm presence of carboxyl group within the samples containing functionalised CNTs. The obtained data confirmed the presence of –COOH group on CNTs by peaks in 1108 to 1438 cm-1 range which disappear in graph of CPQ complex (Fig. **3**) depicting that

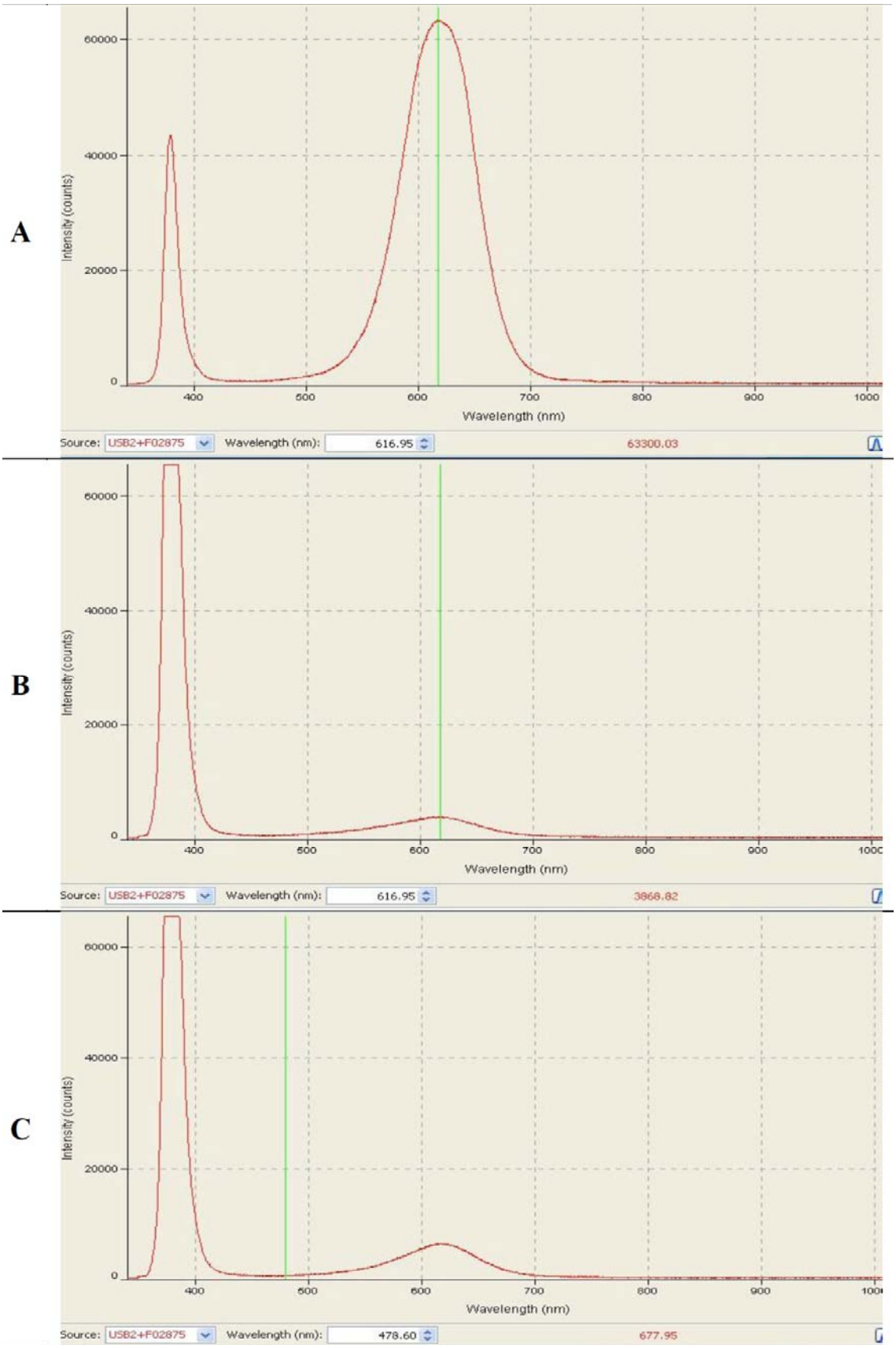

Fig. (2). UV/NIR spectrometry of free QDs (**A**) shows strong emission waveform at 600 nm. This amplitude of waveform diminishes after addition of CNT solution (**B**). The covalently bound CNTs with QDs attached on its surface also dampens the emission waveform (**C**).

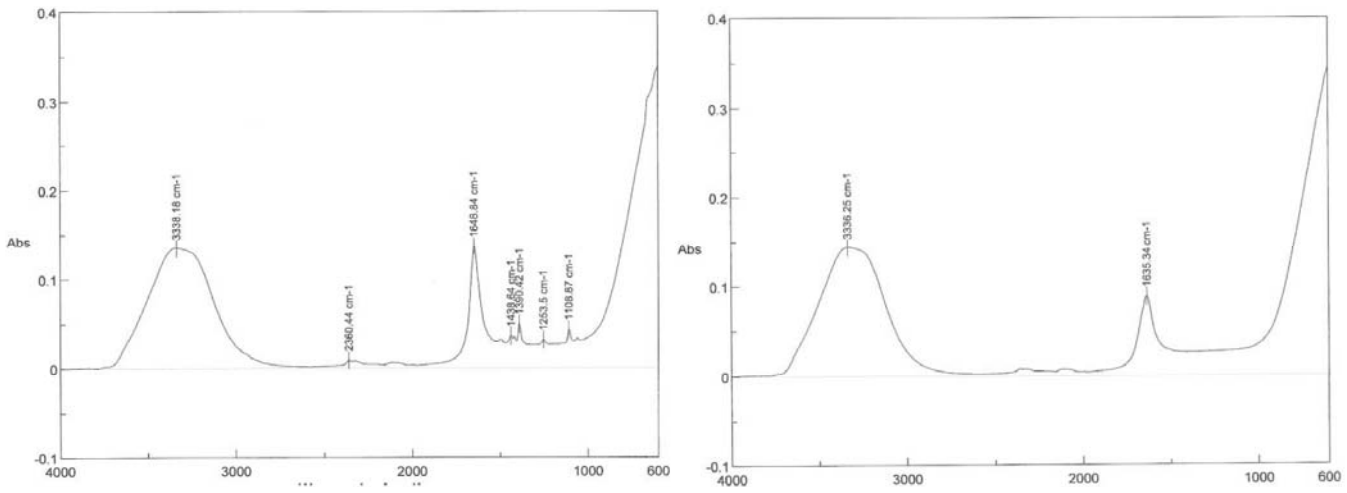

Fig. (3). FTIR spectra analysis showing presence of carboxyl groups of HNO3: H2SO4 treated CNTs (left). The appearances of CPQ complex (right) shows disappearance of CNT waveform suggesting that covalent bonding with polymer has taken place.

carboxyl groups reacted and formed covalent bonds with amine groups of POSS.

Raman Spectrometry

Raman characterisation was performed using InVia Raman microscope (Renishaw®, Wotton-under-Edge, UK). Samples of unbound CNTs, QDs and POSS were studied separately and as compound solution. For comparison, covalently and non-covalently polymer bound SWCNTs were examined. The results demonstrated that in case of covalently bound CNTs, the Raman shift signal somewhat dampened. This finding suggests that CNTs that are pre-functionalised with carboxyl groups become more uniformly covered with POSS rendering them as being more biocompatible (Fig. **4**). The QD sample solution transmitted only weak Raman shift due to the presence of heavy metals within the core; and was not detected in this experiment examining compound CPQ sample. Antibody functionalized complexes were not studied with this method owing to complex nature of proteins which would distort the Raman signal.

Fluorescence Spectrometry

Experiment was performed to examine photobleaching effects of CNTs and POSS on QDs depending on the concentration of the two former. For the experiment 1.5 mL eppendorphs were prepared containing constant 10 mg/mL concentration of QDs. Varied concentrations of CNTs were added to eppendorphs to study photobleaching effects that might result from direct attachment of the two ingredients. The concentrations of CNTs were from 0.1 to 0.9 mg/mL (0.1 mg/mL increments). Same was repeated using varied concentrations of POSS with constant concentrations of QDs. The aim of last part of experiment was to examine photobleaching effects of indirectly attached CNTs to QD, therefore constant concentrations of POSS and QDs were taken, and varied concentrations of CNTs were added in the same manner as before. Fluorescence spectra (FLUOstar optima, BMG LABTECH GmbH, Ortenberg, Germany) were measured at 360 to 590 nm wavelengths from 96-well plates. The samples containing varied concentrations of POSS showed no effect on QD fluorescence according to statistical analysis. Polymer-free CNTs showed significant photobleaching effect on QDs ($p=0.040$) at 0.5 mg/mL concentration. The polymer linked CNTs also proved to have significant impact on QD fluorescence ($p=0.48$), but at higher concentration (Fig. **5**).

Statistical Analysis

The cellular response to components of CNT-QD complex was examined using Alamar blue and DNA assays over three

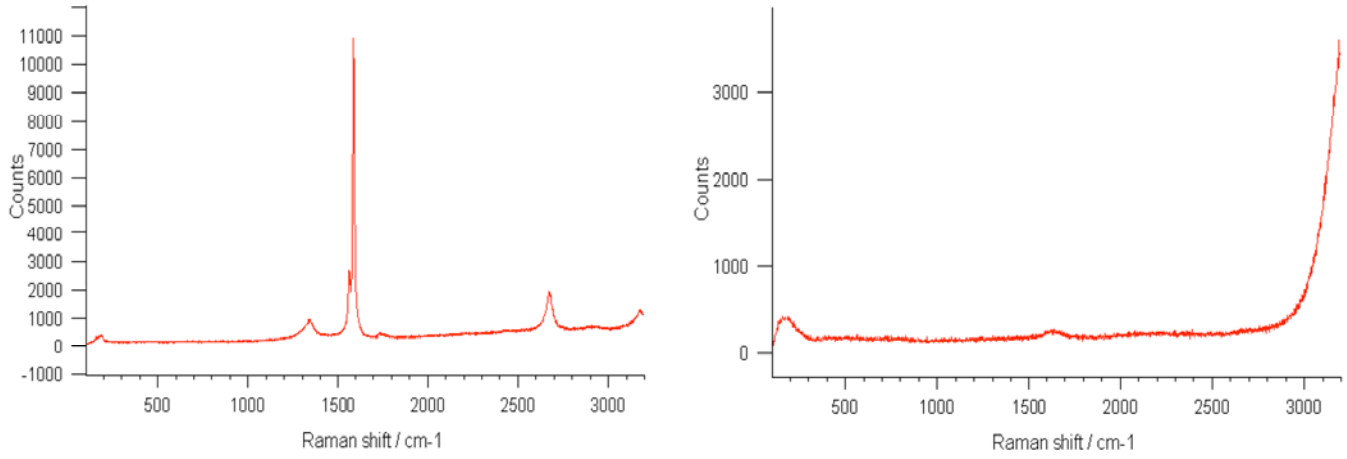

Fig. (4). Raman spectrometry results. Non-covalently bound CNT and POSS (left), the conjugation through ionic bonds is weaker, resulting in poor polymer wrapping around the CNTs; The covalently bound CNT and POSS conjugate (right) formed with strong covalent bonds, CNTs are uniformly wrapped in polymer resulting in weaker Raman shift compared to picture on the left.

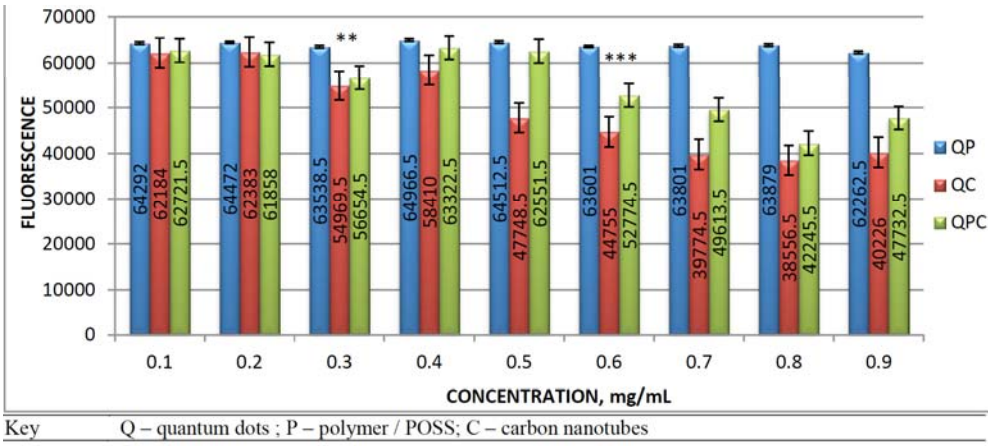

Fig. (5). The quenching effects of QDs using different concentrations of CNTs and POSS examined using fluorescence measurements. POSS did not prove to have significant effect on QD fluorescence. CNTs showed to dampen QD fluorescence significantly (**p=0.04) without the polymer. The POSS linked CNT also showed significant reduction in QD fluorescence (***p=0.048), however the effect was reduced compared to former samples.

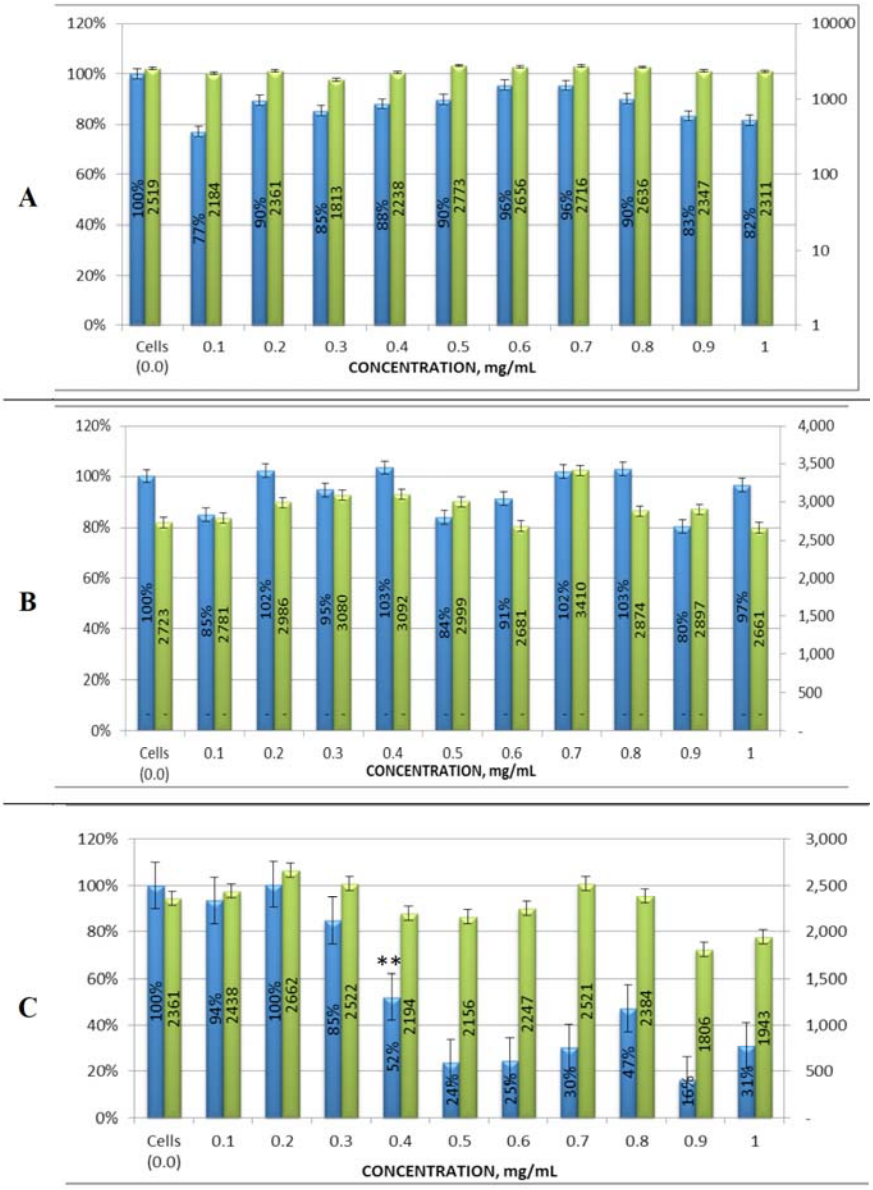

Fig. (6). Graphs of Alamar Blue ( ) and DNA ( ) assays for varied concentrations of POSS, QDs and CNTs. Cell response to neither of concentration of POSS (**A**) or QDs (**B**) was statistically significant. There was significantly reduced (**p=0.040) cell metabolic activity of cells exposed to CNTs (**C**).

consecutive days, and the results were statistically analysed (Fig. **6**). The data were processed by comparing means of the samples against cells in growth media as control using independent-samples Kruskal-Wallis test, and results were considered significant if *p value <0.05*. There was no significant suppression of cell viability with any concentration of polymer, supporting the biocompatible property of octa-ammonium POSS. The analysis of QD effect on cells showed tendency of cell viability suppression, especially on day three, however this was not statistically significant. On contrary, the CNTs showed significant impact on cell metabolic activity (*p=0.040*) at nanotube concentration of 0.4 mg/mL; although the cell proliferation appeared to have tendency to decline with increasing concentrations of CNTs, it did not reach the level of significance.

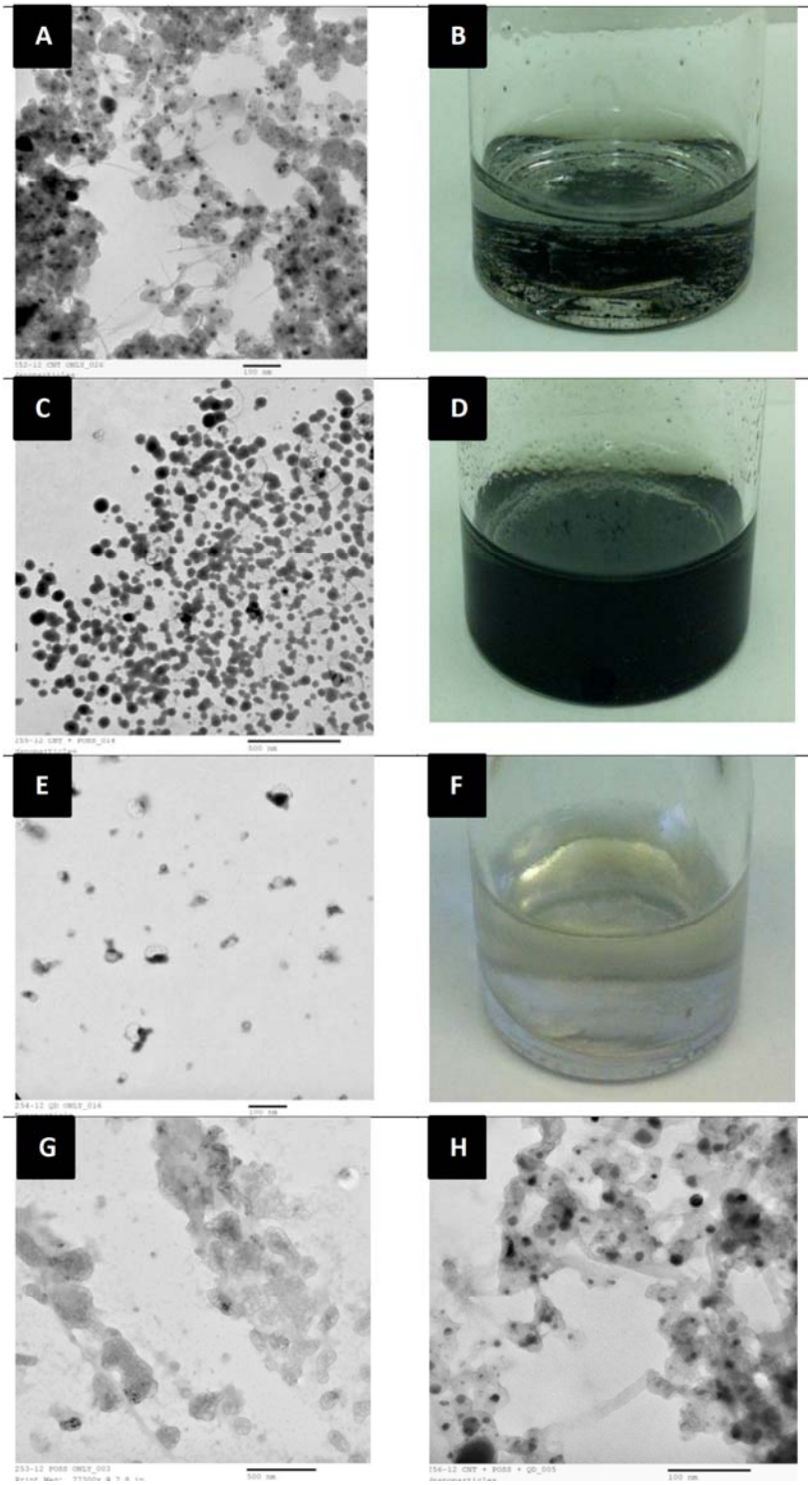

Fig. (7). Transmission electron microscopy images. **A** – carboxyl group functionalised CNT (53000x); **B** – macro-image of (A); **C** – CNTs with POSS (53000x) image demonstrates improved CNT dispersion; **D** – polymer coated CNTs are well dispersed in solvent; **E** – QDs (110000x); **F** – QDs without under day light have slightly discoloured water appearance; **G** – POSS (40000x); **H** – complex of CNTs with covalently bound QDs through attachment of polymer (23000x).

TEM

Transmission electron microscopy images were obtained using Philips CM120 (FEI) apparatus (Eindhoven, Netherlands). This experiment was performed to attain visual proof of QD attachment to CNTs by analysing covalently formed CPQ complex. For comparison, constituents of complex were also studied separately. Owing to their size, unattached QDs were visualised only at high magnification of 110000x, and were difficult to identify in compound solution. A sample of polymer wrapped functionalized CNTs showed visually better dispersion when compared to nanotubes in solvent alone. This corresponded to macro-images of the samples obtained with standard photo camera (Fig. **7**).

Confocal Microscopy

Confocal microscopy (Nikon Eclipse TE300, Japan) was performed at two stages of research; firstly to visualise fluorescence of the components separately and after conjugation, and secondly to observe cellular response to CPQ-antibody complex after 24, 48 and 72 hours of incubation.

Characterisation of CPQ Conjugate

Confocal images of CNT, QD, dried POSS, growth media and mixtures were obtained (Fig. **8**). Dissolved CNTs alone yielded no fluorescence compared to sample of CNT+QD without POSS. In this case QDs were dispersed in no relation to CNTs throughout the solution. The pictures of CPQ complex revealed successful attachment of fluorescent QD to CNTs.

CPQ-antibody Complex and Cells

Cell response was observed on day 1, 2 and 3 after incubation with growth media and CPQ with or without antibodies (Figs. **9**, **10**, **11**). HT29 and PANC1 cancer cell lines were compared to non-cancerous fibroblasts that are not known to express CEA or CA19-9

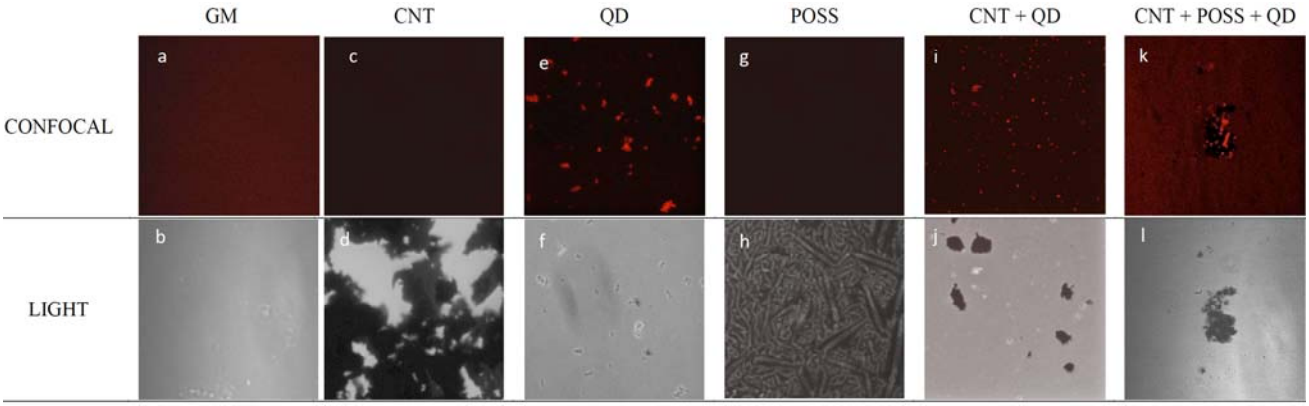

Fig. (8). Images of light and confocal microscopy. **A**,**b** – growth media yields no fluorescence; **c**,**d** – pristine CNTs form clumps; **e**,**d**,**i**,**j** – QDs seen to fluoresce under confocal laser in scattered pattern around CNTs; g,h – dried polymer under light microscopy demonstrates crystalloid appearance, and seems to possess some fluorescent properties; **k**,**l** – CPQ complex shows QDs organised around the CNTs owing to covalent attachment through POSS.

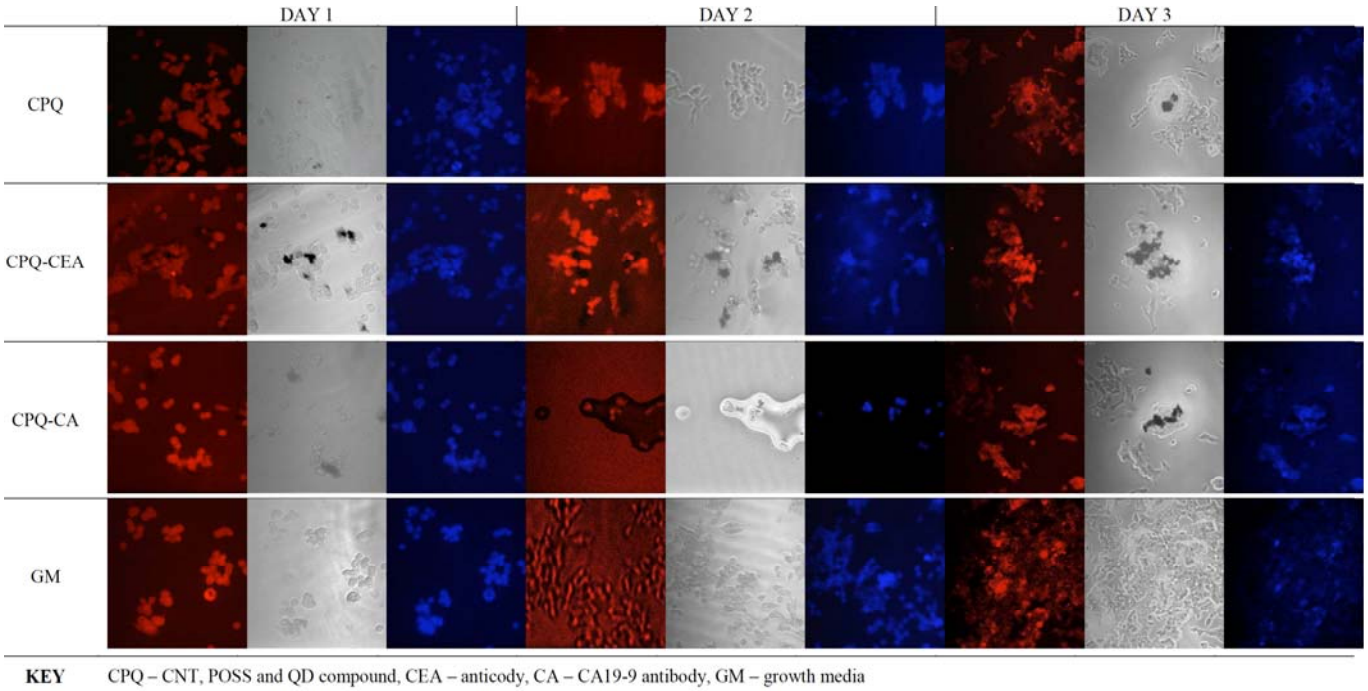

Fig. (9). Images of light and confocal microscopy (laser and UV filters), magnification x40000. HT29 cell morphology over period of three consecutive days when incubated with CPQ compound with or without antibodies. CPQ complexes without antibodies were witnessed to penetrate on day three, in comparison the CPQ with antibody complexes were observed to react with cells already after 24 hours of incubation. The HT29 cells seem to re-stat colonising on day three meaning that higher payloads of treatment are necessary.

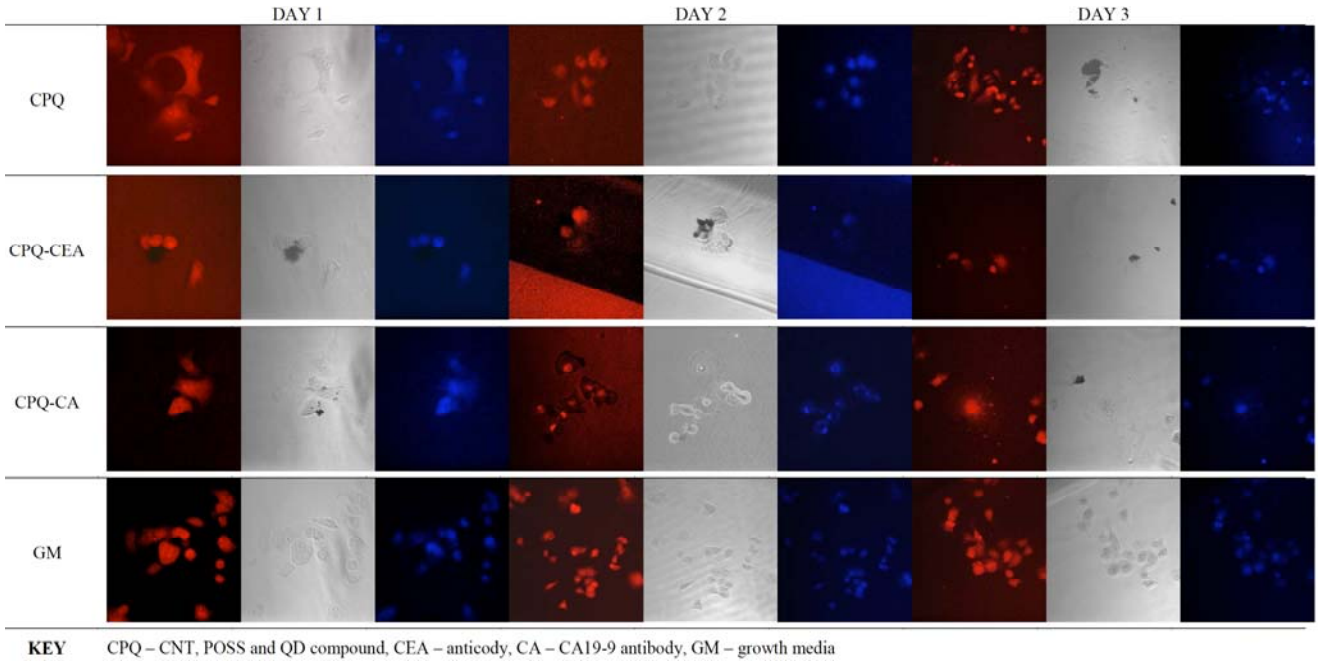

Fig. (10). Light and confocal microscopy images using laser and UV filters, magnification x40000. PANC-1 cell proliferation is markedly supressed from day one in antibody present samples, and continues over period of three days. By day three cells appear to have undergone lysis. The antibody free CPQ samples showed migration of CNTs into the cells only on day three.

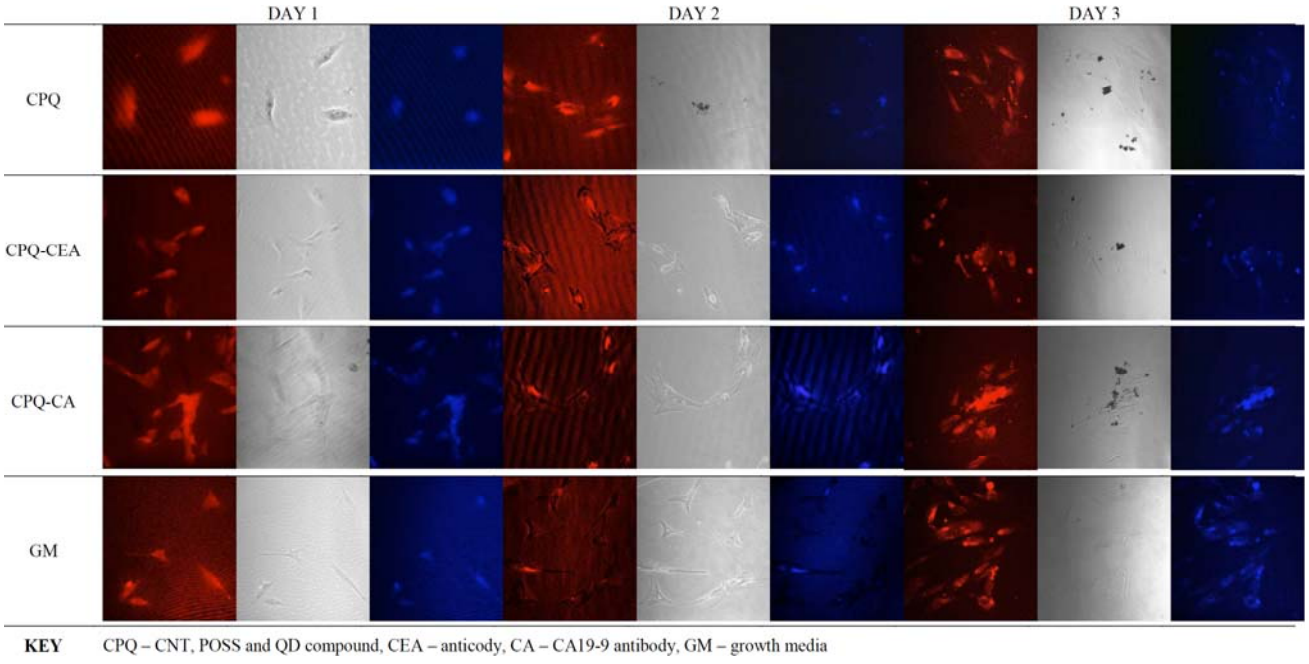

Fig. (11). Images of light and laser and UV filter enhanced confocal microscopy (magnification x40000). 3T3 cell lines show progressive colonisation in all sample groups over the course of three consecutive days. The CNTs have reached the cells on day two in antibody-free sample. The other test samples showed accumulation of CNTs around the fibroblasts only by day three.

antibodies. After 24 hours of incubation, cancer cells were seen attaching to the CPQ-antibody complexes. In contrast, fibroblasts were approaching the complexes only on day three. PANC1 cells treated with CPQ-CEA and CPQ-CA showed deprived growth in both cases progressively over the course of three days by which the time most of the cells have undergone lysis. Similar picture was seen in HT29 cell line; however these cells appeared to gain ability to repopulate on day three. This might show that higher payload of CPQ-antibody is necessary to improve destruction of colonic cancer cells. The QD component of the complex was observed under confocal microscope with the CNTs, albeit the amount of QDs was reduced from expected. This could be due to some of them being internalized into the cell, or that higher concentrations are necessary if the CPQ complexes are to be used for diagnostic purposes. Overall this experiment shows that incorporation of cancer specific antibody improves cancer cell affinity towards CPQ complex, aids earlier uptake into the cells, and results in cell destruction.

DISCUSSION

The commercially available CNTs are materials with admixture of metallic and amorphous carbon particles [25], rendering them unfeasible for work with live tissues and cells. The unpurified form of CNTs is rather inert to chemical reactions due to their insolubility and lack of reactive chemical groups. To overcome this we selected the option to treat CNTs by refluxing them in HNO_3 : H_2SO_4 solution as previously described [26]. This technique removes the CNTs from impurities, improves the solubility factor and provides CNTs with free carboxyl groups on their surface that are chemically active. The FTIR spectrometry confirmed the presence of –COOH groups in our acid treated CNT sample, and enabled further development of the SWCNT-QD compound.

The next step in compound manufacturing involved conjugation of carboxylated CNTs with POSS. The chemical reagents included cross-linkers ED, NHS and DMF. The latter ingredient is very useful for establishment of strong covalent bonding between CNT and the polymer. The effect of using DMF is two-fold. First of all, this enables the 'swelling' of polymer which increases the amine group availability. Secondly, DMF is effective in separating and suspending CNTs [27]. This means that during the stirring phase after addition of DMF, the clumped-up CNTs are better dispersed enabling more uniform coating when polymer is added. From our experiments we derived that ultrasonication is the most crucial step in achieving best quality dispersion at nanoscale level. Before conjugation, the POSS with its eight free $–NH_3$ groups was reacted with the solution of caustic soda (NaOH). This transforms POSS free groups to $–NH_2$ and enables stable conjugation between former and the carboxyl groups on functionalised CNT surface.

The nanotubes in covalently bound CNT-POSS solution appeared well dispersed as compared to the solution of pristine CNTs. This phenomenon was observed over a period of three months; the dispersion quality of POSS coated CNTs remained unchanged over this time period. This outcome was similar to studies performed by different research groups demonstrating that polymers play A major role in enhancing CNT dispersion homogeneity and stability [28, 29]. The satisfactory results of adequate macroscopic dispersion were further supported by TEM analysis which compared solutions of pure and 'polymerised' CNTs, and depicted separation of CNT clumps as an effect of POSS coating. The FTIR analysis showed absent amine groups of POSS after its conjugation with CNTs; this verifies that covalent bonding has taken place between the two components. On the other hand, the carboxyl groups were still identified in solutions of CNT-POSS and CNT-POSS-QD. This is primarily due to high aspect ratio of CNTs resulting in identification of left-over (unreacted) –COOH groups at the tips of nanotubes. And furthermore, this can be explained by the presence of free carboxyl groups on the surface of QDs.

The effect of covalent bonding was also assessed using Raman spectroscopy. The samples of pristine and non-covalently bound CNTs yielded typical Raman spectrum [28, 30] unlike the covalently conjugated sample. In the case of polymer-linked nanotubes the Raman signal appeared to be dampened, which could again be due to more uniform wrapping of the CNTs potentially improving their biocompatibility. Similar findings of distorted Raman shift after covalent binding of nanotubes have been described elsewhere in literature [31].

The QDs were added to the complex *via* the –COOH groups, establishing firm bond with amine groups of the POSS. The UV light emitting property of free QDs was detected as strong signal at 600 nm. The amplitude of signal was reduced to minimum in CNT-QD solution; this undesirable effect disappeared when same experiment was performed on polymer-linked CNT-QD solution. The presence of QDs was also observed with confocal microscopy. The sample of polymer-free CNT-QD solution showed scattered QDs around the clumps of CNTs. Contrary to that, CPQ complex demonstrated that QDs were concentrated around the CNTs thus visually confirming that successful attachment has taken place.

Literature evidence shows that some CNTs are able to emit light at NIR spectrum facilitating their photo-thermal use [30, 32]. Although this project was not designed to evaluate the NIR properties of CNTs, our UV/NIR experiment did not detect the NIR spectrum of CNT sample. A detailed explanation of NIR properties of CNTs is beyond the scope of this project, however, the finding could be related to covalent functionalisation and/or length of the nanotubes [24].

For cell toxicity studies varied concentrations of each ingredient were examined with human colonic cancer cells. The cell response to POSS, QDs and CNTs was assessed with cell proliferation and metabolic activity assays. Statistical analysis of the results confirmed biocompatibility of octa-ammonium POSS with cells, which were observed to behave similarly to those grown in supplemented media only. The dissolved pristine CNTs in contrast produced significant negative effect on cell metabolic activity with as little as 0.4 mg/mL concentration. This highlights the necessity for cautious bio-optimisation of CNTs when used on live cells even at small concentrations. Interestingly, neither of the QD concentrations caused decline in cell proliferation or metabolic activity. This finding will prove useful for further developments of real-time imaging tools as higher payloads of QDs can be used thence improving image quality without hampering well-being of the host. It is worthwhile to remember though, that if QDs are to be used in clinical setting, they should be size-tuned to enable renal clearance and avoid accumulation in RES organs.

After establishing the least toxic concentrations of each ingredient, the CEA and CA9-9 antibodies were added to complete the manufacturing process of CPQ-antibody (CPQ-ab) compound. The presence of antibodies within the CPQ complex was examined using UV-VIS spectrometry; the absorbance peaks at 260 nm wavelengths confirmed this. The final product was then tested on two cancer cell lines and one healthy cell line. Cell behaviour was observed on three consecutive days, and compared using light and confocal microscopy. The QDs were identified under confocal laser beam; however their quantity appeared reduced from anticipated. It might be that their visibility was precluded due to them being internalised into the cell. The other explanation is that higher payload might be necessary for reliable diagnostic imaging studies. And based on our previous on *in vitro* experiments, higher concentrations of QDs are safe, albeit further studies are warranted to confirm this before *in vivo* experiments can be carried out.

An encouraging finding was that internalisation of CPQ-ab complexes appeared to commence from day one in both cancer cell lines, but only after 72 hours in healthy cell line. This inspires to believe that targeted delivery using antibody ligands promotes cancer cell uptake of CPQ complexes when compared to healthy cells. In addition, we found that on third day, HT29 cells restarted to populate. In clinical terms, this could be explained that either higher doses of CPQ-ab compound are needed, or treatment requires repeated cycles of drug administration. For clarification of this, a further study is a necessity to assess cell behaviour over seven days, and supplement to confocal microscopy with cell viability studies.

CONCLUSION

We have successfully described the development process of multifunctional platform for theranostic purpose. A novel covalent binder – ocata-ammonium POSS was used during the manufacturing course, and showed good quality dispersion of CNTs and improved biocompatibility of the complex. Having eight free amine groups,

this polymer offers versatility that we exploited to attach not only CNTs, but also fluorescent moieties – QDs, and tumour specific antibodies. This complex established rapid attachment to the target colonic and pancreatic cancer cells owing to presence of cancer antibodies, resulting in cell internalization of CNTs followed by cell destruction. The control culture of healthy cells also showed internalization of CNTs, but this process was much delayed compared to cancer cells.

An interesting result to bear in mind for further research is the fact that based on metabolic activity and DNA assays performed in this study, the cells failed to show any significant negative response to QDs with concentrations up to 1 mg/mL. This finding can be used for developments of contrast agents and other imaging tools where adequate doses of fluorescent agent are necessary without the risk of harming the host; more evidence, however, is going to be warranted in this regard.

The next prospect would have to establish the fate of CPQ-antibody complex in cell co-cultures or tissue samples. And to advance the research for *in vivo* experiments, drug loading into the CNT core will have to be accomplished. The future studies are necessary to complete the development of this theranostic gadget with ultimate goal to detect early disease in real-time and simultaneous disease elimination.

CONFLICT OF INTEREST

The author(s) confirm that this article content has no conflict of interest.

ACKNOWLEDGEMENTS

Declared none.

REFERENCES

[1] Brakmane G, Winslet M, Seifalian AM. Systematic review: the applications of nanotechnology in gastroenterology. Aliment Pharmacol Ther. 2012; 36(3): 213-21.

[2] Tan A, Madani SY, Rajadas J, Pastorin G, Seifalian AM. Synergistic photothermal ablative effects of functionalizing carbon nanotubes with a POSS-PCU nanocomposite polymer. Journal of nanobiotechnology. 2012; 10(1): 34. Epub 2012/08/02.

[3] Tan A, Yildirimer L, Rajadas J, De La Pena H, Pastorin G, Seifalian A. Quantum dots and carbon nanotubes in oncology: a review on emerging theranostic applications in nanomedicine. Nanomedicine. 2011; 6(6): 1101-14.

[4] Jia G, Wang HF, Yan L, Wang X, Pei RJ, Yan T, *et al.* Cytotoxicity of carbon nanomaterials: Single-wall nanotube, multi-wall nanotube, and fullerene. Environmental Science & Technology. 2005; 39(5): 1378-83.

[5] Madani SY, Naderi N, Dissanayake O, Tan A, Seifalian AM. A new era of cancer treatment: carbon nanotubes as drug delivery tools. International Journal of Nanomedicine. 2011; 6: 2963-79.

[6] Zhang Y, Bai YH, Yan B. Functionalized carbon nanotubes for potential medicinal applications. Drug Discov Today. 2010; 15(11-12): 428-35.

[7] Hu XK, Cook S, Wang P, Hwang HM, Liu X, Williams QL. *In vitro* evaluation of cytotoxicity of engineered carbon nanotubes in selected human cell lines. Science of the Total Environment. 2010; 408(8): 1812-7.

[8] Palomaki J, Valimaki E, Sund J, Vippola M, Clausen PA, Jensen KA, *et al*. Long, Needle-like Carbon Nanotubes and Asbestos Activate the NLRP3 Inflammasome through a Similar Mechanism. Acs Nano. 2011; 5(9): 6861-70.

[9] Murphy FA, Poland CA, Duffin R, Al-Jamal KT, Ali-Boucetta H, Nunes A, *et al.* Length-Dependent Retention of Carbon Nanotubes in the Pleural Space of Mice Initiates Sustained Inflammation and Progressive Fibrosis on the Parietal Pleura. American Journal of Pathology. 2011; 178(6): 2587-600.

[10] Nirmal M, Dabbousi BO, Bawendi MG, Macklin JJ, Trautman JK, Harris TD, *et al.* Fluorescence intermittency in single cadmium selenide nanocrystals. Nature. 1996; 383(6603): 802-4.

[11] Kirchner C, Liedl T, Kudera S, Pellegrino T, MuÃ±oz Javier A, Gaub H, *et al.* Cytotoxicity of colloidal CdSe and CdSe/ZnS nanoparticles. Nano Letters. 2005; 5(2): 331-8.

[12] Smith AM, Duan HW, Mohs AM, Nie SM. Bioconjugated quantum dots for *in vivo* molecular and cellular imaging. Advanced Drug Delivery Reviews. 2008; 60(11): 1226-40.

[13] Gao XH, Yang LL, Petros JA, Marshal FF, Simons JW, Nie SM. *In vivo* molecular and cellular imaging with quantum dots. Current Opinion in Biotechnology. 2005; 16(1): 63-72.

[14] Suri SS, Fenniri H, Singh B. Nanotechnology-based drug delivery systems. J Occup Med Toxicol. 2007; 2: 16. Epub 2007/12/07.

[15] Verdejo R, Jell G, Safinia L, Bismarck A, Stevens MM, Shaffer MS. Reactive polyurethane carbon nanotube foams and their interactions with osteoblasts. Journal of biomedical materials research Part A. 2009; 88(1): 65-73. Epub 2008/02/09.

[16] Ahmed M, Ghanbari H, Cousins BG, Hamilton G, Seifalian AM. Small calibre polyhedral oligomeric silsesquioxane nanocomposite cardiovascular grafts: Influence of porosity on the structure, haemocompatibility and mechanical properties. Acta Biomaterialia. 2011; 7(11): 3857-67.

[17] Desai M, Bakhshi R, Zhou X, Odlyha M, You Z, Seifalian AM, *et al*. A sutureless aortic stent-graft based on a nitinol scaffold bonded to a compliant nanocomposite polymer is durable for 10 years in a simulated *in vitro* model. Journal of endovascular therapy: an official journal of the International Society of Endovascular Specialists. 2012; 19(3): 415-27. Epub 2012/07/14.

[18] Chaloupka K, Motwani M, Seifalian AM. Development of a new lacrimal drainage conduit using POSS nanocomposite. Biotechnology and applied biochemistry. 2011; 58(5): 363-70. Epub 2011/10/15.

[19] Adwan H, Fuller B, Seldon C, Davidson B, Seifalian A. Modifying three-dimensional scaffolds from novel nanocomposite materials using dissolvable porogen particles for use in liver tissue engineering. Journal of biomaterials applications. 2012. Epub 2012/04/26.

[20] Jungebluth P, Alici E, Baiguera S, Le Blanc K, Blomberg P, Bozoky B, *et al*. Tracheobronchial transplantation with a stem-cell-seeded bioartificial nanocomposite: a proof-of-concept study. Lancet. 2011; 378(9808): 1997-2004. Epub 2011/11/29.

[21] Fabbro C, Ali-Boucetta H, Da Ros T, Kostarelos K, Bianco A, Prato M. Targeting carbon nanotubes against cancer. Chem Commun (Camb). 2012; 48(33): 3911-26. Epub 2012/03/20.

[22] Heister E, Neves V, Tilmaciu C, Lipert K, Beltran VS, Coley HM, *et al*. Triple functionalisation of single-walled carbon nanotubes with doxorubicin, a monoclonal antibody, and a fluorescent marker for targeted cancer therapy. Carbon. 2009; 47(9): 2152-60.

[23] Kierny M, Cunningham T, Kay B. Detection of biomarkers using recombinant antibodies coupled to nanostructured platforms. Nano Reviews. 2012; 3.

[24] Liu Z, Tabakman SM, Chen Z, Dai H. Preparation of carbon nanotube bioconjugates for biomedical applications. Nature protocols. 2009; 4(9): 1372-82. Epub 2009/09/05.

[25] Bekyarova E, Ni Y, Malarkey E, Montana V, McWilliams J, Haddon R, *et al*. Applications of Carbon Nanotubes in Biotechnology and Biomedicine. Journal of Biomedical Nanotechnology. 2005; 1(1): 3-17.

[26] Madani SY, Tan A, Dwek M, Seifalian AM. Functionalization of single-walled carbon nanotubes and their binding to cancer cells. International Journal of Nanomedicine. 2012; 7: 905-14.

[27] Dimethylformamide. Wikipedia [updated 28 July 2012 cited 2012 2 July]; Web link]. Available from: http: //en.wikipedia.org/wiki/ Dimethylformamide.

[28] Heister E, Lamprecht C, Neves V, Tilmaciu C, Datas L, Flahaut E, *et al*. Higher Dispersion Efficacy of Functionalized Carbon Nanotubes in Chemical and Biological Environments. Acs Nano. 2010; 4(5): 2615-26.

[29] Yadav S, Mahapatra S, Yoo H, Cho J. Synthesis of multi-walled carbon nanotube/polyhedral oligomeric silsesquioxane nanohybrid by utilizing click chemistry. Nanoscale Research Letters. 2011; 6(1): 122-.

[30] Kam NWS, O'Connell M, Wisdom J, Dai H. Carbon nanotubes as multifunctional biological transporters and near-infrared agents for

selective cancer cell destruction. Proceedings of the National Academy of Sciences of the United States of America. 2005; 102(33): 11600-5.

[31] Liu Z, Tabakman S, Welsher K, Dai H. Carbon Nanotubes in Biology and Medicine: *In vitro* and *in vivo* Detection, Imaging and Drug Delivery. Nano Research. 2009; 2(2): 85-120.

[32] Zhou F, Xing D, Ou Z, Wu B, Resasco D, Chen W. Cancer photothermal therapy in the near-infrared region by using single-walled carbon nanotubes. Journal of biomedical optics. 2009; 14(2): 021009-.

Received: January 11, 2013 Revised: February 21, 2013 Accepted: March 01, 2013